Bioorganic & Medicinal Chemistry Letters 22 (2012) 3001–3005

Contents lists available at SciVerse ScienceDirect

Bioorganic & Medicinal Chemistry Letters

journal homepage: www.elsevier.com/locate/bmcl

Synthesis and evaluation of 1-(substituted)-3-prop-2-ynylureas as antiangiogenic agents

Kingkan Sanphanya [a], Suvara K. Wattanapitayakul [b], Orawin Prangsaengtong [c], Michiko Jo [c], Keiichi Koizumi [c], Naotoshi Shibahara [c], Aroonsri Priprem [d], Valery V. Fokin [e], Opa Vajragupta [a,*]

[a] Department of Pharmaceutical Chemistry, Faculty of Pharmacy, Mahidol University, 447 Sri-Ayudya Rd, Bangkok 10400, Thailand
[b] Department of Pharmacology, Faculty of Medicine, Srinakharinwirot University, 114 Sukhumvit 23, Bangkok 10110, Thailand
[c] Department of Kampo Diagnostics, Institute of Natural Medicine, University of Toyama, 2630 Sugitani, Toyama-shi, Toyama 930-0194, Japan
[d] Department of Pharmaceutical Technology, Faculty of Pharmaceutical Sciences, Khon Kaen University, Khon Kae 40002, Thailand
[e] Department of Chemistry, The Scripps Research Institute, 10550 North Torrey Pines Rd, La Jolla, CA 92037, USA

ARTICLE INFO

Article history:
Received 12 September 2011
Revised 20 January 2012
Accepted 10 February 2012
Available online 22 February 2012

Keywords:
1-(Substituted)-3-prop-2-ynylurea
Cytotoxic agents
Tyrosine kinase inhibitors
EGFR kinase inhibitor
Antiangiogenic agent

ABSTRACT

Novel urea derivatives of alkynes have been designed, synthesized, and evaluated as potential cancer therapeutics leads. The most active 1-((3-chloromethyl)phenyl)-3-prop-2-ynylurea (**1**) exhibited cytotoxic effect against HELA and MCF-7 cell lines with IC_{50} values of 1.55 μM and 1.48 μM, respectively. Further investigation on tube formation assay in human vein umbilical cells (HUVEC) demonstrated that **1** and methyl 4-(3-(3-ethynylureido)benzyloxy) benzoate (**6**) possess antiangiogenic activity, with minimum effective dose of 25 nM (for **1**) and 6.25 μM (for **6**). The ED_{50} of **1** and **6** were found to be 0.26 μM and 17.52 μM, respectively. The results from in vitro tyrosine kinase assay indicated the EGFR inhibition of **1** over other kinases (VEGFR2, FGFR1 and PDGFRβ). The cytotoxicity of **1** against EGFR overexpressing cell line A431 (IC_{50} 36 nM) was comparable to that of erlotinib. The binding mode of **1** from docking simulation in the EGFR active site revealed that the urea motif formed hydrogen bonding with Lys745, Thr854 and Asp855 in hydrophobic pocket of EGFR. Compound **1** is considered as a potential lead for further optimization.

Protein tyrosine kinases (TKs), a family of cell signaling proteins that regulate inter- and intracellular communications, have been implicated in cancer development. Two classes of TKs, categorized by structures, functions and locations, are receptor tyrosine kinases (RTKs) and non-receptor tyrosine kinases (NRTKs). These TKs play an important role in regulation of cell growth, proliferation, differentiation, survival and metabolism.[1,2] RTKs such as vascular endothelial growth factor receptor-2 (VEGFR2), epidermal growth factor receptor (EGFR), fibroblast growth factor receptor-1 (FGFR1), and platelet-derived growth factor receptor (PDGFR) play a key role in angiogenesis, the sprouting process of capillaries from pre-existing vessels. These RTKs are important targets in antiangiogenic drug development. Inhibition of these enzymes can lead to suppression of both cell proliferation and angiogenesis and may become a viable strategy in cancer treatment.[3]

Urea derivatives demonstrate diverse array of biological and pharmacological activities, such as antibacterial, antifungal, anti-inflammatory, antiangiogenic and antiproliferative properties.[4–6] Sorafenib is an example of an anti-proliferative urea agent (Fig. 1).[7–9] It is a tyrosine kinase inhibitor (VEGFR and PDGFR) which was approved by the US FDA for advanced renal cancer.[10]

The 1-(substituted)-3-prop-2-ynylureas, terminal alkynes bearing urea motif, were firstly designed in our lab as an in-house library for the preparation of 1,4-disubsituted-1,2,3-triazole derivatives by copper-catalyzed azide alkyne cycloaddition (CuAAC) reaction.[11]

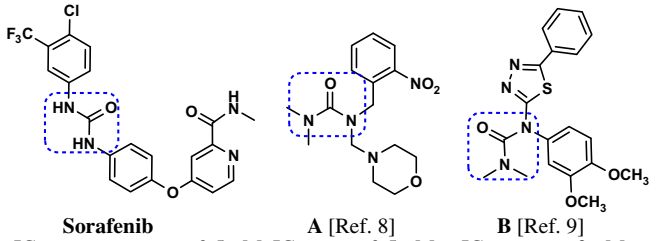

Sorafenib
IC_{50}(MDA-MB-231) = 2.5 μM

A [Ref. 8]
IC_{50} (KB) = 2.5 μM
IC_{50} (K562) = 0.4 μM

B [Ref. 9]
IC_{50} (K562) = 3 μM

Figure 1. Substituted ureas acting as antiproliferative agents. MDA-MB-231, KB and K562 are human breast cancer cell line, human carcinoma of the nosopharynx and human erythroleukemia cell line, respectively.

* Corresponding author. Tel.: +66 26 448 677; fax: +66 26 448 695.
E-mail address: pyovj@mahidol.ac.th (O. Vajragupta).

0960-894X/$ - see front matter © 2012 Elsevier Ltd. All rights reserved.
doi:10.1016/j.bmcl.2012.02.029

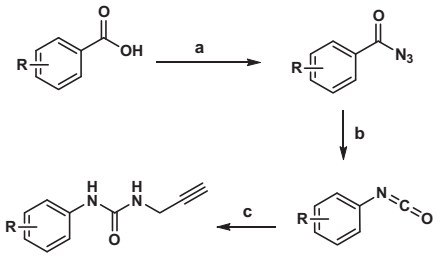

Scheme 1. General synthesis of urea compounds **1**–**5**. Reagents and conditions: (a) DPPA, TEA, toluene or dioxane, rt, 30 min; (b) toluene or dioxane, 100 °C, 1 h; (c) propargylamine, rt, 30 min.

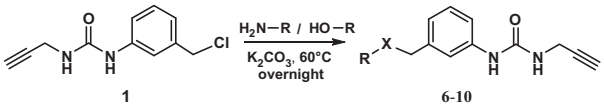

Scheme 2. General synthesis of urea compounds **6**–**10**.

Table 1
Yields and melting points of the synthesized 1-(substituted)-3-prop-2ynylureas

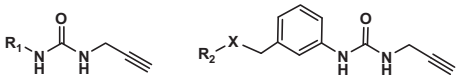

Compoundd	R_1	X	R_2	% Yield	Mp (°C)
1	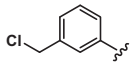	—	—	21.48	158–160
2	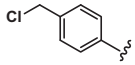	—	—	10.01	132–134
3	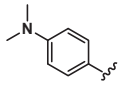	—	—	50.27	178–180
4		—	—	72.48	122–124
5	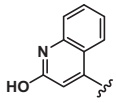	—	—	10.53	246–248
6	—	O	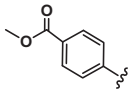	38.12	179–181
7	—	NH		12.23	68–72
8	—	NH	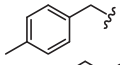	25.53	119–120
9	—	NH	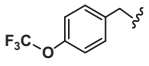	15.34	112–114
10	—	NH	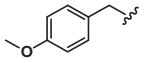	34.87	99–101

The synthesized triazole-based ureas, as well as the azide and alkyne precursors, were screened for their cytotoxic effects against HELA and MCF-7 cell lines. 1-(3-Chloromethyl)-3-prop-2-ynylurea **1** showed cytotoxic effect against HELA and MCF-7.

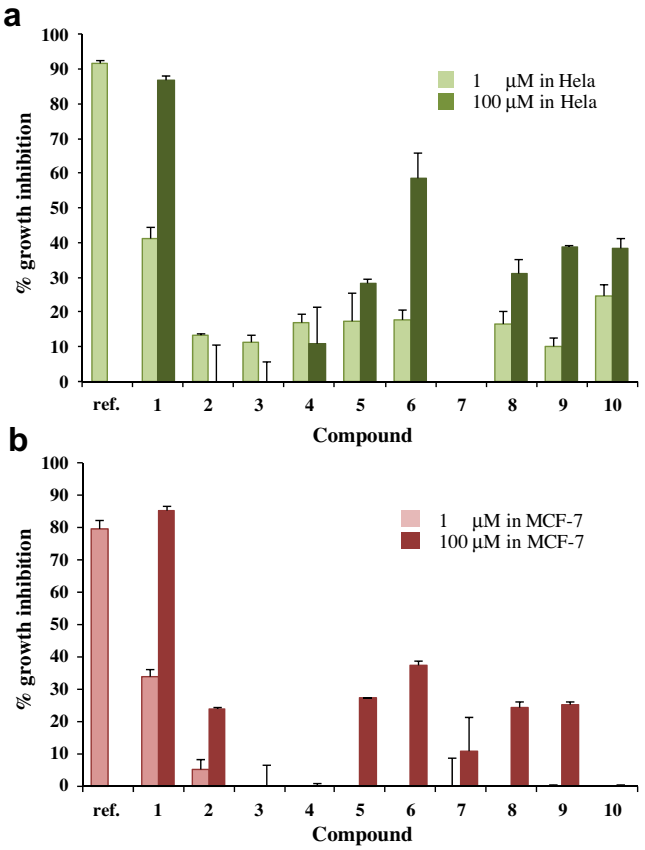

Figure 2. In vitro cytotoxicity effect of 1-(substituted)-3-prop-2-ynylureas at 1 μM and 100 μM against HELA (a) and MCF-7 (b). Doxorubicin at 1 μM was used as reference compound, $n = 3$.

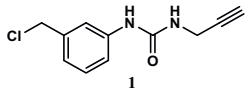

A family of 26 of 1-(substituted)-3-prop-2-ynylureas were next designed by molecular modeling to increase the potency. Flexible ligands were docked to a grid representation of VEGFR2 model derived from crystal structure of the VEGFR2 tyrosine kinase domain in complex with a pyridyl-pyrimidine benzimidazole inhibitor (PDB: 3EWH)[12] using AutoDock4.2[13] (docking experiment and data of all 26 compounds are shown in Supplementary data). Ten compounds were selected based on free energy of binding, hydrogen bond interaction and visual inspection and synthesized and preliminary screened for their cytotoxic effects toward two types of human cancer cell lines, HELA and MCF-7.

Compounds **1**–**5** were prepared by the reaction between various phenyl isocyanates and propargylamine. The synthetic route is illustrated in Scheme 1.[14,15] Various phenyl isocyanates were prepared in situ via Curtius rearrangement of corresponding acyl azides before reacting with propargylamine to give 1-(substituted)-3-prop-2-ynylureas **1**–**5**. Briefly, acyl azides were prepared from the corresponding benzoic acids with diphenylphosphoryl azide (DPPA) in the presence of triethylamine in an appropriate solvent. Then, acyl azides were heated at 100 °C to achieve the corresponding isocyanates that were subsequently reacted with propargylamine yielding the desired compounds **1**–**5**, unoptimized yield: 10–72% (Supplementary data). Compounds **6**–**10** were synthesized by displacement of chloride of compound **1** with phenols or benzylamines in the presence of K_2CO_3 in one step fashion[16] as illustrated in Scheme 2 (unoptimized yield: 17–80%, synthesis

Table 2
IC_{50} values of the cytotoxicity against HELA, MCF-7

Compound	IC_{50}[a] (μM)	
	HELA	MCF-7
1	1.55	1.48
6	12.26	74.87
7	NA[b]	343.48
8	329.10	49.89
9	339.00	282.90
10	391.50	194.90
Doxorubicin	0.19	0.06

[a] Mean values of three independent experiments are reported.
[b] No activity.

Table 3
IC_{50} against the HUVEC

Compound	IC_{50}[a] (μM)	
	Primary	EA.hy926
1	20	10.54
6	100	78.23
7	50	191.72

[a] Mean values of three independent experiments are reported.

details are shown in Supplementary data). All synthesized compounds were displayed in Table 1.

The synthesized 1-(substituted)-3-prop-2-ynylureas **1**–**10** were then tested for their cytotoxic effects at 1 and 100 μM against HELA and MCF-7 using MTT assay[17] (Supplementary data). Doxorubicin was used as reference. The compounds that showed growth inhibition over 30% at 100 μM against either cancer cell line were selected for IC_{50} determination.

The initial screening results at two-point concentration of compounds **1**–**10** were shown in Figure 2. Concentration dependent cytotoxic effects of the compounds in this series against HELA and MCF-7 were observed. Although all compounds demonstrated poor cytotoxic activities comparing to doxorubicin, compound **1** exhibited substantial cytotoxic effect at 100 μM against both HELA and MCF-7 (growth inhibitions of 86.86% and 85.16% for HELA and MCF-7, respectively). Data from cytotoxicity assay of compounds **1**–**5** suggested that both size and position of substituents on 1-(substituted)-3-prop-2-ynylurea greatly affected on cytotoxic properties of the compounds in this series. Substituents on *para*-position of 1-(phenyl)-3-prop-2-ynylurea decreased cytotoxic effect regardless of the size of substituents as observed in compounds **2** and **3**. Bulky substituent that is, fused ring at position 1 of urea motif (compound **5**) also suppressed cytotoxic potency. The extended structure of compound **1** by displacement of chloride moiety with various phenyl or benzyl via ether- or amine-linker (compounds **6**–**10**) did not enhance anticancer activity as anticipated, even deteriorated. These emphasized the influence of size of the substituent on phenyl ring at position 1 of urea motif on the cytotoxicity.

Compounds **1**, **6** and **8**–**10** showed % growth inhibition over 30% at 100 μM against either or both HELA and MCF-7 were selected for the determination for IC_{50}. Among the compounds in this series, compound **1** is most potent compound showing cytotoxic effect on both HELA and MCF-7 with IC_{50} of 1.55 μM and 1.48 μM, respectively (Table 2).

Compounds **1** and **6** showing the best activity against two cancer cell lines were further evaluated for their antiangiogenic effects by tube formation assay, regardless of the considerably high cytotoxic IC_{50} in μM level. Compound **7** with poor activity was included in the assay for comparison. Tube formation assays were performed at non-cytotoxic doses of each compound against the human vein umbilical cell line (HUVEC) (Supplementary data). To identify non-cytotoxic doses for tube formation assay, the in vitro cytotoxicity of compounds **1**, **6** and **7** against HUVEC were performed by MTT assay in the similar fashion as of HELA and MCF-7. IC_{50} values of selected compounds against HUVEC were listed in Table 3.

Tube formation assays of compounds **1**, **6** and **7** were performed. Comparing with control, both compounds **1** and **6**

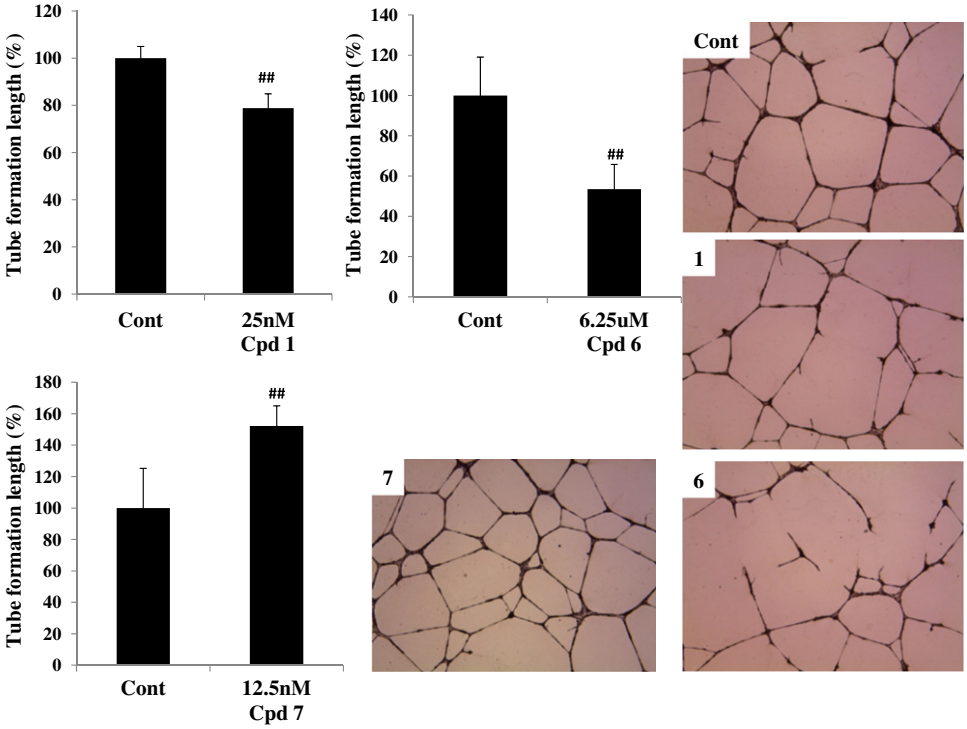

Figure 3. Effect of compounds **1**, **6** and **7** on tube formation comparing with control, $n = 3$, $^{**}p < 0.01$.

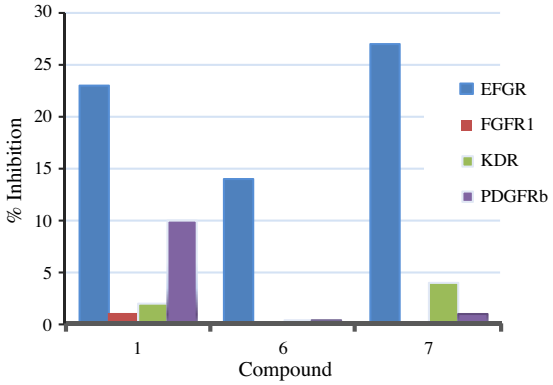

Figure 4. Kinase inhibitory profile at 1 μM against EGFR, FGFR1, VEGFR2 and PDGFRβ tyrosine kinases, % inhibition of erlotinip at 1 μM against EGFR was 98%.

significantly suppressed tube formation of HUVEC. The half maximal effective concentration (EC_{50}) of compounds **1** and **6** against tube formation were found to be 0.26 μM and 17.52 μM, respectively. The observed results from tube formation assay indicated that compounds **1** and **6** possessed antiangiogenic properties against HUVEC. The IC_{50}:ED_{50} ratios for HUVEC of compounds **1** and **6** were 77 and 6, respectively. The antiangiogenic ED_{50} dose of compound **1** was 77 times lower than its cytotoxic IC_{50} dose while that of compound **6** was only 6 times. Apparently, compound **1** did not only possess more potent antiangiogenic activity but also showed safer profile than compound **6**. The minimum effective doses were also determined at the non-cytotoxic dose, compounds **1** and **6** significantly suppressed tube formation of HUVEC at 25 nM and 6.25 μM with 21.18% and 46.47% inhibition, respectively (Fig. 3). Interestingly, compound **7** at non-cytotoxic dose (12.5 nM) showed the increase in tube formation, this compound is currently under investigation for its molecular mechanism.

Compounds **1** and **6** exhibiting significant antiangiogenic activity were evaluated for their effects on tyrosine kinases involving in angiogenesis. In vitro kinase assay of compounds **1** and **6** at 1 μM against VEGFR2, FGFR1, EGFR and PDGFRβ were performed. The levels of phosphorylation of the tyrosine kinase-specific ligand peptides[18–21] at 1 μM of test compounds were measured (Supplementary data). The kinase inhibition profile was displayed in Figure 4.

The tested compounds predominantly inhibited EGFR tyrosine kinase more than other kinases. At 1 μM, compound **1** exhibited significant activity against EGFR and PDGFRβ while compounds **6** and **7** inhibited EGFR tyrosine kinase only. The better cytotoxicity of compound **1** may be due to its ability to inhibit two kinases, EGFR and PDGFRβ.

Since compounds **1** and **6** inhibited EGFR more than the intended VEGFR2, docking of these compounds into ATP binding site of EGFR was performed using AutoDock4.2 to simulate a binding model. The EGFR model was derived from crystal structure of erlotinib bound EGFR obtained from RCSB (PDB: 1M17).[22] Dock poses

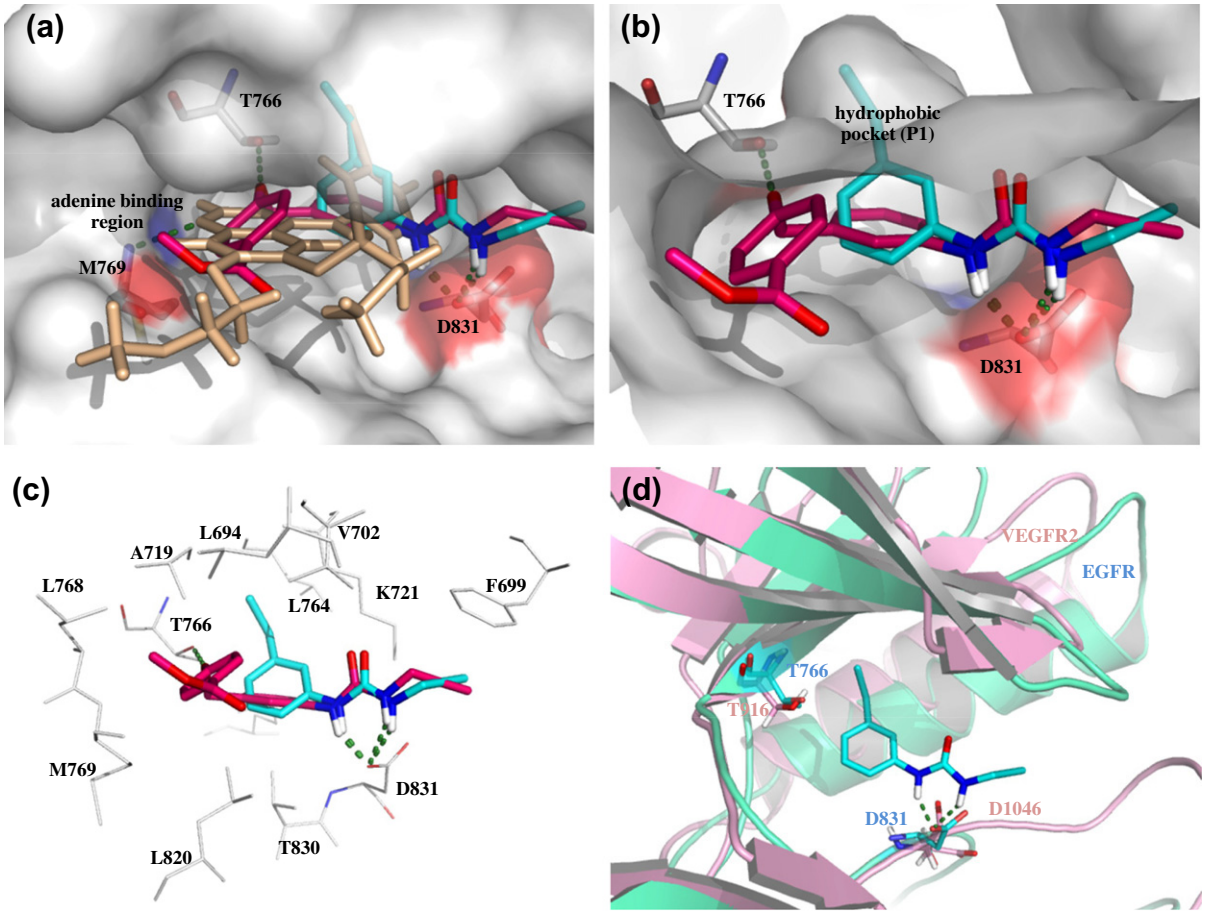

Figure 5. (a) Overlay of binding models of 1-(substituted)-3-prop-2-ylnylurea **1** (cyan), **6** (magenta) and erlotinib (wheat) in kinase domain of EGFR, (b) Overlay of **1** and **6** and their H-bond interactions in the EGFR active site (green dot line), **1** occupied back cavity of ATP binding site of EGFR (P1), (c) binding modes of **1** and **6** displaying interacted amino acid residues, (d) overlay binding model of compound **1** in kinase domain of EGFR (blue) and VEGFR2 (pink), key amino acid residues for H-bond interactions (observed in compounds **1** and **6**) in EGFR (T766 and D831) and in VEGFR2 (T916 and D1046) were illustrated.

Table 4
IC_{50} against A431 cell lines

Compound	IC_{50} (nM)
1	36.00
6	215.50
7	318.00
Erlotinib	55.50

of these compounds were compared with crystal pose of erlotinib as shown in Figure 5a.

EGFR docking results showed that 1-(substituted)-3-prop-2-ynylureas **1** and **6** partially occupied the ATP binding pocket of EGFR whereas erlotinib extensively occupied EGFR kinase domain (Fig. 5a). The partial occupancy may explain the observed low potency in kinase inhibition of these compounds. The 3-chloromethylphenyl substituent of **1** penetrated deeply in the back cavity of the ATP which was a poorly conserved hydrophobic area of the ATP binding site of EGFR.[23] This part of structure was surrounded by the hydrophobic side chains of Phe699, Val702, Ala719, Leu764, Leu820 and the hydrophobic parts of Lys721, Thr766 and Thr830. The urea motif established two hydrogen bonds with the carboxylate of conserved Asp831, a component of DFG motif in the beginning of the activation loop of EGFR which involved in Mg-ATP binding[24] (Fig. 5b). The occupied location of compound **6** was similar to those of **1**, two hydrogen bonds between both *H*N of urea and *CO*OH of Asp831, and an extra hydrogen bond between oxygen atom of ether and O*H* of Thr766, gatekeeper residue of EGFR (Fig. 5b). In addition to Thr766 and Asp831, amino acid residues in hydrophobic pocket that involved hydrophobic interaction included Leu694, Phe699, Val702, Ala719, Lys721, Leu764, Leu768, Met769, Leu820 and Thr830 (Fig. 5c). The binding mode cannot explain the higher potency of **1** over **6** since **6** showed more interacted hydrogen bonds over **1**. The overlay binding mode of **1** in kinase domain of EGFR and VEGFR2 was displayed in Figure 5d. Compound **1** also occupied back cavity of VEGFR2 and was surrounded by the hydrophobic side chains of Val848, Phe1047, Leu1049 and the hydrophobic part of Arg842, Lys868, Asp1046 and Asp1052 (data not shown). The observed hydrogen bond interactions cannot explain the selectivity of **1** against EGFR over VEGFR2 since **1** located in the similar region and bound to DFG motif of both kinases (Asp831 of EGFR and Asp1046 of VEGFR2). However, sequence alignment between EGFR (PDB: 1M17) and VEGFR2 (PDB: 3EWH) by Needle (EMBOSS)[25] showed 28.6% identity and 44.4% similarity suggested that the difference in the hydrophobic component of back cavity observed between EGFR and VEGFR2 might be the key factor controlling the selectivity of **1** and **6** against EGFR over VEGFR2; which appeared to be consistent with the reported notion.[23]

As compounds **1** and **6** were found to inhibit different kinases, especially EGFR, the effect on human epidermoid carcinoma cells A431, EGFR overexpressing cell lines[26–29] was performed (Supplementary data) and the IC_{50} values were reported in Table 4. The IC_{50} values in nM level for EGFR overexpressing A431 cells demonstrated the significance of EGFR kinase inhibition as those for HUVEC were in μM level. The cellular cytotoxicity of **1** was comparable to erlotinip despite of moderate EGFR kinase inhibition, it was possibly due to its ability to inhibit two kinases, EGFR and PDGFRβ.

In summary, a series of novel 1-(substituted)-3-prop-2-ynylureas based on structural modification of compound **1** were prepared to increase the binding capability. The structural modifications of **1** with extended aromatic side chains to increase the binding capability did not enhance tyrosine kinase inhibition nor antiproliferative as expected. Compounds **1** and **6** were cytotoxic against human cancer cells and demonstrated antiangiogenic effect in vitro. In EGFR overexpressing cell line (A431), the cytotoxicity of compound **1** was in nM level comparable to that of erlotinip. The binding mode of **1** from EGFR docking simulation demonstrated that the smaller in size of **1** facilitates and accommodates the hydrogen bond formation in the active sites of the receptors as evidenced by the inhibition of two types of tyrosine kinases (EGFR and PDGFRβ). The urea motif in the compound plays an important role in hydrogen bond interaction with amino acid residues in the active binding site. Terminal alkyne containing urea motif can be considered as new scaffold for further optimization of a potential cancer therapeutic lead.

Acknowledgments

This work was supported by the Royal Golden Jubilee Ph.D. Program (RGJ Grant No. PHD/0229/2547) funded by Thailand Research Fund (TRF) and the commission of Higher Education Thailand (CHE-RG 2551). The authors thank Dr. Benjamin Fraser and Dr. Neil P. Grimster for their valuable advice in some synthesis reactions.

Supplementary data

Supplementary data associated with this article can be found, in the online version, at doi:10.1016/j.bmcl.2012.02.029.

References and notes

1. Zwick, E.; Bange, J.; Ullrich, A. *Trends Mol. Med.* **2002**, *8*, 17.
2. Culhane, J.; Li, E. *US Pharm.* **2008**, *33*, 3.
3. Zwick, E.; Bange, J.; Ullrich, A. *Endocr. Relat. Cancer* **2001**, *8*, 161.
4. Li, H.-Q.; Lv, P.-C.; Yan, T.; Zhu, H.-L. *Anticancer Agents Med. Chem.* **2009**, *9*, 471.
5. Tale, R. H.; Rodge, A. H.; Hatnapure, G. D.; Keche, A. P. *Bioorg. Med. Chem. Lett.* **2011**, *21*, 4648.
6. Zheng, Q.-Z.; Cheng, K.; Zhang, X.-M.; Liu, K.; Jiao, Q.-C.; Zhu, H.-L. *Eur. J. Med. Chem.* **2010**, *45*, 3207.
7. Yao, P.; Zhai, X.; Liu, D.; Qi, B. H.; Tan, H. L.; Jin, Y. C.; Gong, P. *Arch. Pharm. Chem. Life Sci.* **2010**, *343*, 17.
8. Li, H. Q.; Zhu, T. T.; Yan, T.; Luo, Y.; Zhu, H. L. *Eur. J. Med. Chem.* **2009**, *44*, 453.
9. Ahirwar, K. *IJPRD* **2011**, *2*, 209.
10. Drugs@FDA.
11. Rostovtsev, V. V.; Green, L. G.; Fokin, V. V.; Sharpless, K. B. *Angew. Chem., Int. Ed.* **2002**, *41*, 2596.
12. Cee, V. J.; Cheng, A. C.; Romero, K.; Bellon, S.; Mohr, C.; Whittington, D. A.; Bak, A.; Bready, J.; Caenepeel, S.; Coxon, A.; Deak, H. L.; Fretland, J.; Gu, Y.; Hodous, B. L.; Huang, X.; Kim, J. L.; Lin, J.; Long, A. M.; Nguyen, H.; Olivieri, P. R.; Patel, V. F.; Wang, L.; Zhou, Y.; Hughes, P.; Geuns-Meyer, S. *Bioorg. Med. Chem. Lett.* **2009**, *19*, 424.
13. http://autodock.scripps.edu/.
14. Flynn, D. L.; Kaufman, M. D.; Patt, W. C.; Petillo, P. A. USA Patent WO/2008/034008A2, 2008.
15. Spraul, B. K.; Suresh, S.; Jin, J.; Smith, D. W. *J. Am. Chem. Soc.* **2006**, *128*, 7055.
16. Clark, P. G.; Day, M. W.; Grubbs, R. H. *J. Am. Chem. Soc.* **2009**, *131*, 13631.
17. IC_{50} value is the concentration required to inhibit 50% of cell viability by the test compound after exposure to cells.
18. Itokawa, T.; Nokihara, H.; Nishioka, Y.; Sone, S.; Iwamoto, Y.; Yamada, Y.; Cherrington, J.; McMahon, G.; Shibuya, M.; Kuwano, M.; Ono, M. *Mol. Cancer Ther.* **2002**, *1*, 295.
19. Mohammadi, M.; McMahon, G.; Sun, L.; Tang, C.; Hirth, P.; Yeh, B. K.; Hubbard, S. R.; Schlessinger, J. *Science* **1997**, *276*, 955.
20. Weber, W.; Bertics, P. J.; Gill, G. N. *J. Biol. Chem.* **1984**, *259*, 14631.
21. Baxter, R. M.; Secrist, J. P.; Vaillancourt, R. R.; Kazlauskas, A. *J. Biol. Chem.* **1998**, *273*, 17050.
22. Stamos, J.; Sliwkowski, M. X.; Eigenbrot, C. *J. Biol. Chem.* **2002**, *277*, 46265.
23. Zuccotto, F.; Ardini, E.; Casale, E.; Angiolini, M. *J. Med. Chem.* **2009**, *53*, 2681.
24. Hubbard, S. R.; Till, J. H. *Annu. Rev. Biochem.* **2000**, *69*, 373.
25. The tool for pairwise sequence alignment from European Bioinformatics Institute (EMBL-EBI) at http://www.ebi.ac.uk/Tools/psa/emboss_needle.html.
26. Gan, H. K.; Walker, F.; Burgess, A. W.; Rigopoulos, A.; Scott, A. M.; Johns, T. G. *J. Biol. Chem.* **2007**, *282*, 2840.
27. Kwok, T. T.; Sutherland, R. M. *Br. J. Cancer* **1991**, *64*, 251.
28. Rigerike, T.; Blystad, F. D.; Levy, F. O.; Madshus, I. H.; Stang, E. *J. Cell Sci.* **2002**, *115*, 1331.
29. Bravo, R.; Burckhardt, J.; Curran, T.; Müller, R. *EMBO J.* **1985**, *4*, 1193.